Available online at www.sciencedirect.com
SCIENCE DIRECT®
Thermochimica Acta 412 (2004) 85–90
thermochimica acta
www.elsevier.com/locate/tca

The heat capacity of Au_2S(cr) at low temperatures and derived thermodynamic functions

V.M. Gurevich [a], K.S. Gavrichev [b,*], V.E. Gorbunov [b], N.N. Baranova [a], B.R. Tagirov [c,d], L.N. Golushina [b], V.B. Polyakov [a]

[a] *Vernadsky Institute of Geochemistry and Analytical Chemistry RAS, 19 Kosygina Str., Moscow 117195, Russia*
[b] *Kurnakov Institute of General and Inorganic Chemistry RAS, Laboratory of Chemical Thermodynamics, 31 Leninsky Prosp., Moscow 119991, Russia*
[c] *Institute Geology of Ore Deposit, Petrography, Mineralogy and Geochemistry RAS, 35 Staromonetnyi Per, Moscow 119017, Russia*
[d] *Géochimie: Tranferts et Mécanismes, CNRS (UMR 5563)-OMP, 38 rue des Trente-Six Ponts, Toulouse 31400, France*

Received 7 February 2003; received in revised form 4 September 2003; accepted 4 September 2003

Abstract

The heat capacity of synthetic crystalline gold sulfide, Au_2S, was determined from 14 to 309 K. Fitting of the heat capacity curve yields the following values of the standard thermodynamic properties at 298.15 K and 1 bar: $C^0_{p,m}$=83.54 ± 0.15 J K^{-1} mol^{-1}, $\Delta_0^{298}S^0_m$ = 139.22 ± 0.77 J K^{-1} mol^{-1}, and $\Delta_0^{298}H^0_m$ = 17.591 ± 0.041 kJ mol^{-1}.

Keywords: Thermodynamic properties; Adiabatic calorimetry; Heat capacity; Entropy; Gold sulfide

1. Introduction

This paper represents a part of work studying thermodynamic properties of solid phases in the Ag–Au–S system using low-temperature adiabatic calorimetry and solid state galvanic cell technique. Literature data demonstrate that Au_2S is a metastable solid phase [1]. However, its thermodynamic properties are of high importance for physical chemistry and geochemistry. Au_2S was used by Renders and Seward [2] and Zotov et al. [3] to determine the stability of aqueous complexes $AuHS^0_{(aq)}$ and $Au(HS)_2{}^-$, which predominate in sulfide bearing natural fluids. Accordingly, accuracy of the standard thermodynamic properties for these important aqueous species is directly related to the uncertainty in the thermodynamic data for Au_2S. These thermodynamic data are also necessary to develop a thermodynamic model for "invisible gold" dispersed in the crystalline structure of natural sulfides (see, for example, [4] and references therein).

Crystalline structure of gold sulfide was characterized by Hirch et al. [5], Ishikawa et al. [6] performed X-ray powder diffraction spectra at 80–450 K. It was determined that Au_2S belongs to the isometric–hexoctahedral crystal system (space group *Pn*3*m*, lattice spacing a = 5.02057 Å) with a cuprite-type structure. No structural change or phase transition was found in this temperature range. Au_2S was found to be stable in air up to 370 K but decompose over 420–490 K. Electrical conductivity and electromotive force measurements performed in [6] demonstrated that Au_2S is a p-type semiconductor. Barton [1] determined entropy of Au_2S 147.1 J K^{-1} mol^{-1} from the temperature dependence of the constant of exchange reaction between electrum and Au–Ag sulfide solid solution. This entropy value differs by 11.8 J K^{-1} mol^{-1} from the estimate of Barton and Skinner [7] (158.9 J K^{-1} mol^{-1}). No direct measurement of the heat capacity of Au_2S was carried out earlier.

The aim of the present study is to measure the heat capacity of Au_2S at 14–309 K and determine its standard entropy.

2. Experimental

2.1. Synthesis and characterization of Au_2S

99.99% gold and "for analysis" reagents KCN, HCl, NH_4OH, and CS_2 were used for the synthesis. Au_2S was

* Corresponding author. Tel.: +7-95-9542911; fax: +7-95-9541279.
E-mail address: guskov@igic.ras.ru (K.S. Gavrichev).

0040-6031/$ – see front matter © 2003 Elsevier B.V. All rights reserved.
doi:10.1016/j.tca.2003.09.002

prepared as described in [2]. Briefly, this method consisted in reacting 1 g of metallic gold with 10 ml of aqua regia on water bath. The obtained solution was evaporated under stirring to form wet salts but not to dryness. Then, 50 ml of bidistilled H_2O and 10 ml of concentrated NH_4OH were added to the residue to form fulminating gold approximate composition $Au(NH_3)_3(OH)_3$. The excess of NH_4OH was removed by heating on the water bath during several hours. After cooling, the product was filtered through middle porosity filter and washed several times with hot distilled water. Obtained wet product was dissolved in a KCN solution (3 g of KCN in 80 ml of bidistilled H_2O) which was then bubbled with H_2S during 1 h. Finally, heavy black precipitate of Au_2S was deposited from this solution by addition of ~5 ml of concentrated HCl with subsequent heating to the temperature slightly below the boiling point. After cooling, the formed precipitate was washed with bidistilled H_2O, ethanol, diethyl ether and with CS_2 to remove S_2, and then again with dietyl ether, ethanol and water to remove organic solvents. The product was dried several days over P_2O_5 and kept in the dark.

The synthesis product was checked for homogeneity, composition and particle size using X-ray powder diffraction, thermogravimetry and electron microscopy techniques. XRD analyses were performed with a DRON-3 X-ray powder diffractometer using a Cu Kα radiation. XRD peaks position of the product corresponded to the pattern of Au_2S given in [5,6] with the most intensive peaks at *d* (Å) = 2.88(10), 2.51(8), 1.770(7), 1.444(5), and 1.515(3). No crystalline gold and sulfur were detected. Thermogravimetric analysis was performed in air with the heating rate of 10 K min^{-1}. Sample started to decompose at 443 K and its weight stabilized at about 573 K. The observed weight loss was 7.7 ± 0.5%. This value is close to the sulfur content in Au_2S (7.53 wt.%). Scanning electron microscopy analyses were performed on a JSM-5300 analytical scanning electron microscope with energy dispersive spectrometer Link ISIS. These analyses demonstrated that the synthesized Au_2S is a homogeneous powder with the particle size of about 300 nm. Concentration of elements other than Au and S in the synthesized sulfide was within the detection limit of this method (~0.2–0.5%).

2.2. Calorimetry

Adiabatic calorimeter used for the heat capacity measurements is described in detail in [8]. The heat capacity measurements were performed in the temperature range of 14.09–303.33 K by step-wise technique using the 2 cm^3 stainless steel calorimetric ampoule. The sample weight was 2.96645 g.

3. Results and discussion

The experimental molar heat capacity values are listed in Table 1 for molecular mass of Au_2S $M = 425.9986\ g\ mol^{-1}$ [9], and plotted in Fig. 1. In the present study, ADE-type equation [10] was used to approximate experimental data on heat capacity

$$C_p^0(T) = a_0 T (C_v)^2 + n\left[a_1 D_1\left(\frac{\theta_1}{T}\right) + a_2 D_2\left(\frac{\theta_2}{T}\right) + a_3 D_3\left(\frac{\theta_3}{T}\right) + a_4 E\left(\frac{\theta_E}{T}\right)\right] \quad (1)$$

Table 1
Experimental heat capacities of Au_2S(cr) (J K^{-1} mol^{-1}) ($M = 425.993\ g\ mol^{-1}$)

T (K)	$C^0_{p,m}$	T (K)	$C^0_{p,m}$	T (K)	$C^0_{p,m}$	T (K)	$C^0_{p,m}$
14.09	6.09	65.12	44.91	129.61	60.73	212.71	75.43
15.56	7.20	68.30	45.87	133.66	61.89	217.87	76.35
16.78	10.34	71.36	47.04	137.67	62.50	223.27	77.00
18.42	12.42	74.41	47.57	141.73	63.28	228.73	77.41
20.45	15.05	77.43	48.11	145.74	64.15	233.96	78.19
22.29	19.07	80.44	49.17	149.73	64.93	239.24	78.67
24.37	21.25	83.47	49.86	153.66	65.75	244.47	78.96
26.71	24.09	86.54	50.60	157.66	66.66	249.94	79.37
29.24	25.65	89.53	51.20	161.81	67.38	255.30	80.10
31.80	27.76	92.49	51.91	165.97	68.04	260.64	80.62
34.62	29.97	95.46	52.57	170.10	69.13	264.06	80.61
37.46	31.95	98.43	53.71	174.88	70.16	270.12	81.40
40.36	33.78	101.41	53.95	180.08	70.79	275.45	81.93
43.27	35.33	104.40	54.82	185.32	71.79	280.92	81.96
46.08	36.75	107.41	55.57	190.48	72.81	286.65	82.73
48.86	37.98	110.42	56.51	195.71	73.36	292.72	83.11
51.12	39.53	113.46	57.07	197.34	73.77	298.60	83.90
55.26	41.44	117.36	57.98	198.68	73.36	303.93	84.00
58.55	42.68	121.37	58.59	202.24	74.23	309.33	84.07
62.04	44.14	125.44	59.87	207.52	74.85		

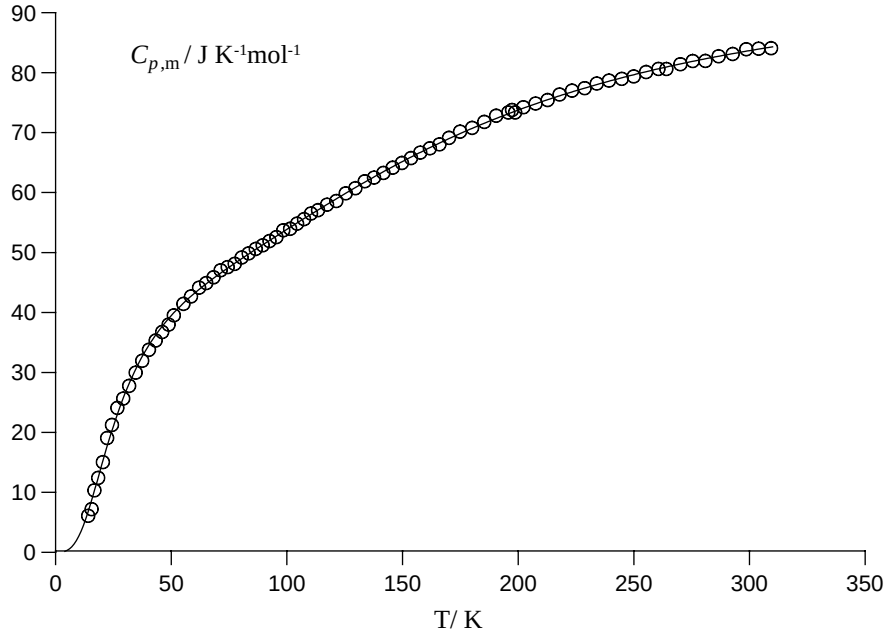

Fig. 1. Molar heat capacity of Au_2S as a function of temperature. Points correspond to experimental data. The curve was calculated using Eq. (1) with parameters listed in the last column of Table 2.

where n is the number of atoms in a molecule (for Au_2S $n = 3$) and E the Einstein function

$$E\left(\frac{\theta_E}{T}\right) \equiv 3R\frac{(\theta_E/T)^2\exp(\theta_E/T)}{(\exp(\theta_E/T)-1)^2} \quad (2)$$

D is the one-dimensional Debye function

$$D\left(\frac{\theta}{T}\right) \equiv 3R\left(\frac{\theta}{T}\right)^{-3}\int_0^{\theta/T}\xi^4\frac{\exp\xi}{(\exp\xi-1)^2}\mathrm{d}\xi \quad (3)$$

θ_1, θ_2, θ_3, and θ_E are characteristic temperatures of the Debye and the Einstein functions, respectively, and a_0, a_1, …, a_4 are linear coefficients. The $C_v(T)$ function is written as

$$C_v = n\left[a_1D_1\left(\frac{\theta_1}{T}\right) + a_2D_2\left(\frac{\theta_2}{T}\right) + a_3D_3\left(\frac{\theta_3}{T}\right) + a_4E\left(\frac{\theta_E}{T}\right)\right] \quad (4)$$

Coefficients and characteristic temperatures in Eq. (1) were calculated using the two-step procedure:

1. Preliminary analysis showed that measurements were not of equal accuracy in ranges of 14.09–51.12 K and 51.12–309.33 K. The scatter of experimental points is one order of magnitude larger in the range of 14.09–51.12 K than at higher temperatures. To take into account this fact in our further calculations, it is needed to evaluate dispersions of measurements in temperature ranges mentioned above separately. For this purpose, the Eq. (1) was used in the range of 51.12–309.33 K. In the range of 14.09–51.12 K, contribution of Einstein's term and difference between C_p and C_V are negligible and the following can be used

$$C_p^0(T) = n\left[a_1D_1\left(\frac{\theta_1}{T}\right) + a_2D_2\left(\frac{\theta_2}{T}\right) + a_3D_3\left(\frac{\theta_3}{T}\right)\right] \quad (5)$$

Values of parameters a_1, …, a_3, θ_1, …, θ_3 in Eq. (4) and a_0, …, a_4, θ_1, …, θ_E in Eq. (1) were found by non-linear least-square method (*LSM*). We used the descent procedure to minimize the dispersion:

$$\sigma^2 = \frac{\sum_{i=1}^{k}(\Delta C_{pi})^2}{k} \quad (6)$$

where ΔC_{pi} is deviation of the experimental point from the Eq. (1) or (5); k is the number of experimental points in first range or second range. The calculation technique is described in [11,12]. Values of a_i, θ_i, and σ^2 are listed in the first and second columns of Table 2.

2. On the second step, the non-linear *LSM* is used for the total temperature range of measurements 14.09–309.33 K. The dispersions calculated on the first step of calculations were used as weight factors on this step. We minimized the weighted dispersion

$$\sigma^2 = \frac{\sum_{i=1}^{k}(\Delta C_{pi})^2 w_i}{k} \quad (7)$$

The weight factors w_i were equal to unity for experimental points in range of 51.12–309.33 K temperature range and equal to $(\sigma^2)_{51-309\,K}/(\sigma^2)_{14-51\,K} = 0.089$ for experimental points in range of 14.09–51.12 K. The technique of calculations is analogous to that used on step 1

Table 2
Values of adjustable parameters in Eqs. (1) and (5)

Parameter	Temperature range (K)		
	14.09–51.12 (Eq. (5))	51.12–309.33 (Eq. (1))	14.09–309.33 (Eq. (1))
a_0 (J^{-1} mol)	–	0.34225×10^{-6}	0.34839×10^{-6}
a_1	1.1503	1.1503	1.1503
a_2	0.8170	0.8170	0.8170
a_3	0.8170	0.8170	0.8170
a_4	–	0.3333	0.3333
θ_1 (K)	106	104	105
θ_2 (K)	124	128	127
θ_3 (K)	1173	557	556
θ_E (K)	–	657	658
σ_2 ($J^2\,K^{-2}\,mol^{-2}$)	0.45	0.040	0.042

[12,13]. Calculated parameters a, θ, and σ^2 are given in the last column of Table 2.

The values of thermodynamic functions calculated using these parameters from 0 to 309 K are listed in Table 3. Calculations result in the following values of the standard heat capacity, entropy and enthalpy change of Au_2S(cr) at $T = 298.15$ K: $C^0_{p,m} = 83.54 \pm 0.15\,J\,K^{-1}\,mol^{-1}$, $\Delta^{298}_0 S^0_m = 139.22 \pm 0.77\,J\,K^{-1}\,mol^{-1}$, and $\Delta^{298}_0 H^0_m = 17.591 \pm 0.041\,kJ\,mol^{-1}$. Uncertainties of these values were estimated using the method described in [12]. Difference between experimental data and the fitting curve (Eq. (1)) as well as uncertainties of experimental C^0_p values are shown in Fig. 2.

3.1. The extrapolation of the $C^0_{p,m}(T)$ function from 50 K to the absolute zero using Eq. (1)

Often, heat capacity data in helium range (below 50 K) are absent. The typical problem arising in this case is to extrapolate experimental data to 0 K. We suggest the *ADE* equation (Eq. (1)) for this purpose. Here, we demonstrate extrapolation properties of the *ADE* equation using the Au_2S as an example. One can find some more details of the extrapolation procedure in [14] where experimental data [15] on γ-La_2S_3 heat capacity and our data on Sb_2S_3 heat capacity are used.

We calculated the fitting parameters in Eq. (1) by the technique described above using the experimental data in the range of 51.12–309.33 K only. The results of these

Table 3
Thermodynamic properties of Au_2S(cr) at selected temperatures

T (K)	$C^0_{p,m}$ ($J\,K^{-1}\,mol^{-1}$)	$\Delta^T_0 S^0_m$ ($J\,K^{-1}\,mol^{-1}$)	$\Delta^T_0 H^0_m$ ($J\,mol^{-1}$)	T (K)	$C^0_{p,m}$ ($J\,K^{-1}\,mol^{-1}$)	$\Delta^T_0 S^0_m$ ($J\,K^{-1}\,mol^{-1}$)	$\Delta^T_0 H^0_m$ ($J\,mol^{-1}$)
4	0.174	0.0580	0.174	100	53.86	63.65	3340
6	0.589	0.197	0.895	110	56.28	68.90	3891
8	1.39	0.466	2.81	120	58.64	73.90	4465
10	2.68	0.905	6.81	130	60.92	78.68	5063
12	4.47	1.54	13.9	140	63.11	83.28	5683
14	6.70	2.40	25.0	150	65.19	87.70	6325
16	9.24	3.45	40.9	160	67.14	91.97	6987
18	11.93	4.70	62.1	170	68.98	96.09	7667
20	14.65	6.09	88.7	180	70.69	100.09	8366
25	21.07	10.07	178.3	190	72.28	103.95	9080
30	26.48	14.40	297.6	200	73.76	107.70	9811
35	30.84	18.82	441.3	210	75.13	111.33	10555
40	34.33	23.18	604.6	220	76.40	114.86	11313
45	37.15	27.38	783.5	230	77.57	118.28	12083
50	39.48	31.43	975.3	240	78.65	121.60	12864
55	41.47	35.29	1177	250	79.66	124.84	13656
60	43.19	38.97	1389	260	80.58	127.98	14457
65	44.76	42.49	1609	270	81.44	131.04	15267
70	46.20	45.86	1836	280	82.24	134.01	16086
75	47.56	49.09	2071	290	82.98	136.91	16912
80	48.87	52.21	2312	298.15	83.54	139.22	17591
85	50.14	55.21	2559	300	83.67	139.74	17745
90	51.40	58.11	2813	310	84.31	142.49	18585
95	52.64	60.92	3074				

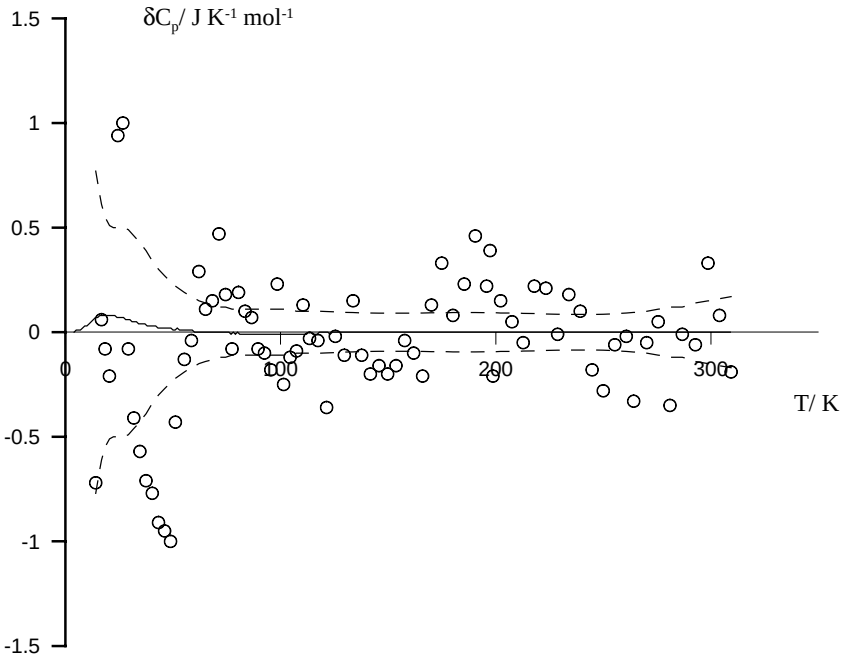

Fig. 2. Uncertainties and deviations of experimental C_p^0 values from fitting curve. Circles (○) corresponds to deviations of experimental points from the fitting curve (1) in the range of 14.09–309.33 K (base line). Dashed lines (- - -) show ±2σ interval calculated at the 95% confidence level. Solid line (—) corresponds to deviations of the curve calculated using C_p^0 values in the range of 51.12–309.33 K from that calculated using C_p^0 values in the range of 14.09–309.33 K. Parameters of the curves listed in second and third columns of Table 2.

Table 4
Entropies and enthalpy increments of Au_2S(cr) at 50 and 298.15 K evaluated by Eq. (1) using experimental data in 14.09–309.33 and 51.12–309.33 K for computing *ADE* equation parameters

Range of approximation (K)	$\Delta_0^{50} S_m^0$ (J K^{-1} mol^{-1})	$\Delta_0^{298} S_m^0$ (J K^{-1} mol^{-1})	$\Delta_0^{50} H_m^0$ (kJ mol^{-1})	$\Delta_0^{298} H_m^0$ (kJ mol^{-1})
14.09–309.33	31.43	139.22	0.975	17.591
51.12–309.33	31.53	139.32	0.977	17.593

calculations are listed in Table 2, where the results of calculations using data in the total range of 14.09–309.33 K are also presented. A comparison (see also Fig. 2) shows close agreement between both sets of calculated C_p^0 values. Deviations of calculated C_p^0 values from experimental data do not exceed the experimental error. A good agreement can be observed also for $\Delta_0^T S_m^0$ and $\Delta_0^T H_m^0$ at temperatures 50 and 298.15 K (Table 4). Based on these results, we conclude that *ADE* equation (Eq. (1)) may be successfully used for extrapolation of the $C_{p,m}^0$ experimental data from 50 to 0 K for solids of the analogous crystal system.

Acknowledgements

We are grateful to M. Thibaut for XRD and thermogravimetric analyses of Au_2S, Oksana Kyznetsova for top quality XRD analyses of Au_2S samples, and A. Mokhov for SEM analyses.

Financial support was provided by RFBR grant 03-05-64804 and Russian Science Support Foundation to BRT.

References

[1] M.D. Barton, Econ. Geol. 75 (1980) 303–316.
[2] P.I. Renders, T.M. Seward, Geochim. Cosmochim. Acta 53 (1989) 245–253.
[3] A.V. Zotov, N.N. Baranova, L.N. Bannykh, Geochem. Int. 31 (1996) 216–221.
[4] G. Simon, S.E. Kesler, S. Chryssoulis, Econ. Geol. 94 (1999) 405–421.
[5] H. Hirch, A. Cugnac, M. Gadet, J. Pouradier, Comput. Rend. Acad. Sci. Ser. B 263 (1966) 1328–1330.
[6] K. Ishikawa, T. Isonaga, S. Wakita, Y. Suzuki, Solid State Ionics 79 (1995) 60–66.
[7] P.B. Barton Jr., B.J. Skinner, Ore mineral stabilities, in: H.L. Barnes (Ed.), Geochemistry of Hydrothermal Ore Deposits, second ed., Wiley, New York, 1979, pp. 278–403.
[8] V.E. Gorbunov, V.M. Gurevich, K.S. Gavrichev, Russ. J. Phys. Chem. 56 (1982) 149–151.

[9] R.D. Loss, IUPAC comossion on atomic weights and isotopic abundances, Chem. Int. 23 (2001) 179.
[10] V.M. Gurevich, K.S. Gavrichev, V.E. Gorbunov, Geochem. Int., 2003, in press.
[11] V.M. Gurevich, V.E. Gorbunov, K.S. Gavrichev, I.L. Khodakovsky, Geochem. Int. 37 (1999) 423–434.
[12] V.M. Gurevich, K.S. Gavrichev, V.E. Gorbunov, T.V. Danilova, L.N. Golushina, I.L. Khodakovsky, Geochem. Int. 39 (2001) 1007–1014.
[13] V.M. Gurevich, K.S. Gavrichev, V.E. Gorbunov, T.V. Danilova, L.N. Golushina, Geochem. Int. 39 (2001) 676–682.
[14] V.M. Gurevich, K.S. Gavrichev, V.E. Gorbunov, E.V. Busheva, L.N. Golushina, G.A. Bergman, Geochem. Int. 40 (2002) 164–172.
[15] E.F. Westrum, R. Burriell, J.B. Gruber, P.E. Palmer, B.J. Beaudry, B.A. Plautz, J. Chem. Phys. 91 (1989) 4838–4848.